Science of the Total Environment 630 (2018) 502–516

Contents lists available at ScienceDirect

Science of the Total Environment

journal homepage: www.elsevier.com/locate/scitotenv

SWAT-MODSIM-PSO optimization of multi-crop planning in the Karkheh River Basin, Iran, under the impacts of climate change

Majid Fereidoon *, Manfred Koch

Department of Geotechnology and Geohydraulics, University of Kassel, 34125 Kassel, Germany

HIGHLIGHTS

- SWAT hydrologic model was built and calibrated/ validated on observed river streamflow
- Projected climate data were generated using quantile mapping method
- Projected river discharge was estimated using future climate variables and calibrated-SWAT
- An integrated economic water management model was developed consisting of a combination of SWAT-LINGO-MODSIM-PSO (SLMP)
- Optimal areas under cultivation are computed by the SLMP, with the aim of maximizing the total annual benefits.

GRAPHICAL ABSTRACT

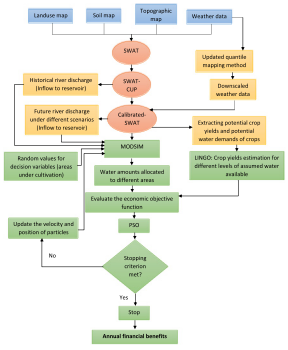

ARTICLE INFO

Article history:
Received 29 September 2017
Received in revised form 22 January 2018
Accepted 19 February 2018
Available online 24 February 2018

Editor: Ouyang Wei

Keywords:
SWAT-LINGO-MODSIM-PSO
Optimization
Agricultural benefit
Climate change
Karkheh basin, Iran

ABSTRACT

Agriculture is one of the environmental/economic sectors that may adversely be affected by climate change, especially, in already nowadays water-scarce regions, like the Middle East. One way to cope with future changes in absolute as well as seasonal (irrigation) water amounts can be the adaptation of the agricultural crop pattern in a region, i.e. by planting crops which still provide high yields and so economic benefits to farmers under such varying climate conditions. To do this properly, the whole cascade starting from climate change, effects on hydrology and surface water availability, subsequent effects on crop yield, agricultural areas available, and, finally, economic value of a multi-crop cultivation pattern must be known. To that avail, a complex coupled simulation-optimization tool SWAT-LINGO-MODSIM-PSO (SLMP) has been developed here and used to find the future optimum cultivation area of crops for the maximization of the economic benefits in five irrigation-fed agricultural plains in the south of the Karkheh River Basin (KRB) southwest Iran. Starting with the SWAT distributed hydrological model, the KR-streamflow as well as the inflow into the Karkheh-reservoir, as the major storage of irrigation water, is calibrated and validated, based on 1985–2004 observed discharge data. In the subsequent step, the SWAT-predicted streamflow is fed into the MODSIM river basin Decision Support System to simulate and optimize the water allocation between different water users (agricultural, environmental, municipal and industrial) under standard operating policy (SOP) rules. The final step is the maximization of the economic benefit in the five agricultural plains through constrained PSO (particle swarm optimization) by adjusting the cultivation areas (decision variables) of different crops (wheat, barley, maize and "others"), taking into account their specific prizes and optimal crop yields under water deficiency, with the latter computed in the LINGO-sub-optimization module embedded in the SLMP-tool. For the optimization of the agricultural benefits in the KRB in the near future (2038–2060), quantile-mapping (QM) bias-corrected downscaled predictors for daily precipitation and temperatures of the HadGEM2-ES GCM-model under RCP4.5- and RCP8.5-emission scenarios are used as climate drivers in

* Corresponding author.
E-mail address: majid.fereidoon@gmail.com (M. Fereidoon).

https://doi.org/10.1016/j.scitotenv.2018.02.234
0048-9697/© 2018 Elsevier B.V. All rights reserved.

the streamflow- and crop yield simulations of the SWAT-model, leading to corresponding changes in the final outcome (economic benefit) of the SLMP-tool. In fact, whereas for the historical period (1985–2004) a total annual benefit of 94.2 million US$ for all multi-crop areas in KRB is computed, there is a decrease to 88.3 million US$ and 72.1 million US$ for RCP4.5 and RCP8.5, respectively, in the near future (2038–2060) prediction period. In fact, this future income decrease is due to a substantial shift from cultivation areas devoted nowadays to high-price wheat and barley in the winter season to low-price maize-covered areas in the future summers, owing to a future seasonal change of SWAT-predicted irrigation water available, i.e. less in the winter and more in the summer.

© 2018 Elsevier B.V. All rights reserved.

1. Introduction

Out of all global resources, water is definitely the most important and invaluable one, as it is used for many purposes, such as drinking, agricultural irrigation, and industrial process (Zhou et al., 2002; Altunkaynak et al., 2005). Population growth and boosting of living standards have increased the demands for fresh water all across the world over the last decades. Regarding agricultural water use, 70% of the freshwater withdrawals from surface and groundwater are consumed for the production of crops (Molden, 2007). Above factors are putting the future status of water availability in question. The situation is, not to the least, exacerbated by climate change, namely, in those regions of the world which are already suffering from water scarcity nowadays. In fact, as climate change affects temperature, precipitation and the water cycle, in general, (Allen and Ingram, 2002; Lenderink and Van Meijgaard, 2010; Reder et al., 2016), its strongest important impact will be on agriculture (Fischer et al., 2005; Khan et al., 2009; Calzadilla et al., 2010), especially in semi-arid and arid areas with already limited natural water resources. Changing climate variables like temperature, precipitation patterns and concentration of carbon dioxide in the atmosphere will impact other water budget variables, such as evapotranspiration, streamflow, soil moisture and snow water equivalent, all of which will directly or indirectly affect the crop production (Kang et al., 2009).

The economic aspects of the agriculture sector contribution to the gross domestic product (GDP) play an important role in many countries of the world, particularly, in developing countries. This agricultural economic contribution is almost 23.4% in Pakistan (Usman, 2016) and estimated to be around 10% in Iran (Madani et al., 2016). Since the water use in irrigated agriculture in these developing or emerging countries is, because of limited technical knowledge and poor pricing of the real economic value of water, generally inefficient and the available water resources are limited (Molle and Berkoff, 2009), it is very important for water engineers and policy-makers to develop schemes for optimal water allocation which take into account the various trade-offs between economic, social and environmental impacts. For example, in Iran, where agriculture depends mainly on irrigation, the economic return on water use in this sector is rather low and crop patterns in most areas of the country are inappropriate and incompatible with the regional water availability conditions (Zare and Koch, 2014; Madani et al., 2016). Agricultural economists have by now developed various economic approaches or models for representing and bringing together agricultural water allocations and demands by evaluating, for example, the responses of water use to water price for agricultural crops, i.e. what is called the price elasticity of the water demand (Moore et al., 1994; Hendricks and Peterson, 2012). However, as these models are often purely economic, they do not always take into account appropriately the complicated local hydrological conditions and constraints, i.e. the physics of the agricultural water resources system. To overcome this deficiency, one has to invoke combined models of hydrological prediction and optimization. Such (constrained) optimization models – the constraints are computed by the hydrological model - for water allocation are just starting to come to the fore and appear to be useful tools to improve the efficiency of water use, to determine optimal cropping pattern and, so eventually, to maximize economic benefits. Sethi et al. (2006) developed linear programming methodologies for irrigated and rain-fed agricultures and crops in a coastal region in India, in order to allocate agricultural land and water resources seasonally for maximization of the net annual benefit. Wang et al. (2015) used an optimal water resources allocation model in the Heihe river basin located in the arid northwest region of China to attain maximum economic, social and ecological benefits, while considering land-use change of the past 20 years. There have also been some applications of optimization techniques for agriculture water resources allocation in Iran. Zare and Koch (2014) used also a linear programming technique for the optimization of cultivation pattern with the aim to maximize farmer's profits in an irrigated land in a semi-arid area of Iran. Banihabib et al. (2016) proposed an optimization model for annual water allocation to maximize the total economic benefit among the agricultural, industrial and service sectors in a combined 19,000 km^2 - large area of Tehran and Alborz Provinces, Iran. Furthermore, Zare and Koch (2017) determined the optimal agricultural irrigation water allocation from conjunctive water sources, in the agriculturally important Miandarband plain, Iran, by coupling a PSO (particle swarm optimization) model with a hybrid Wavelet/ANFIS-fuzzy C-means (FCM) simulation model.

The Karkheh River Basin (KRB) which is located in a semi-arid to arid part of Iran is a good example of an agriculturally heavily exploited basin with typical water challenges the whole country and other regions all around the world are faced with in a similar manner. KRB, as the third largest and the most productive river basin in Iran, is known as the “food basket of Iran”, but has been constantly facing water scarcity in recent years (Ahmad and Giordano, 2010), notwithstanding the fact, that the availability of irrigation water in the downstream section of the basin has increased tremendously over the last 15 years with the construction and termination of the Karkheh reservoir (KR) at the beginning of this century (Fereidoon and Koch, 2017). Nevertheless, due to imminent climate change in the region - IPCC climate change scenarios predict that the average temperature in Iran will rise by 1.5–4.5 °C, if the CO_2-concentration doubles by the year 2100 (Amiri and Eslamian, 2010) - the future agricultural production in the KRB may not be fully guaranteed. In fact, Ashraf Vaghefi et al. (2015) analyzed climate change impacts on wheat production by coupling the SWAT hydrological model (Arnold et al., 1998; Neitsch et al., 2002) – which provides the hydrologic and water resources information based on climate drivers – with the MODSIM decision support system for prioritized water allocation (Labadie, 1995) and came up with a table of options for three different crop scenarios describing the areal extents of wheat production in the basin and the ensuing water deficits, as well as the energy production from the Karkheh dam. However, as these authors did not consider the optimization of cropping patterns with regard to an economic analysis, the present study aims to just do that, by setting up a coupled simulation-optimization tool SWAT-LINGO-MODSIM-PSO (SLMP) to finally determine the optimal crop pattern which maximizes the total annual benefits of the farmers in the region under various climate change scenarios for the region.

The article is organized as follows: After description of the study area and the modeling procedures used, firstly, the SWAT model for estimating river discharge and inflow to the Karkheh reservoir (KR) is

calibrated and validated. Secondly, the projected inflow to the KR is estimated using downscaled climate data for future climate scenarios as input to the calibrated SWAT-model. Thirdly, SWAT–estimated KR-inflows are entered into the MODSIM water allocation model to build a reservoir-irrigation system model for the downstream section of the KRB. Finally, an optimal cropping pattern simulation-optimization model is set up for the baseline- and future scenarios using the coupled MODSIM-PSO model, where areas under cultivation are considered as decision variables, to maximize the total annual benefits from the irrigated crops in five agricultural regions downstream of the KR.

2. Study area

The KRB is located in southwest Iran (Fig. 1), between 30°58–34°56 N latitude and 46°06–49°10 E longitude, and is, with an area of 50,700 km^2, the third largest watershed of that country (Qureshi et al., 2010). Nearly 60% of the KRB lies in within mountainous regions, where and surface and ground water resources are replenished from winter snow falls in the high Zagros mountain range. The KRB constitutes 9% of the whole irrigated area of Iran and provides approximately 10% of the country's total wheat production (Marjanizadeh et al., 2010). The climate of the KRB is characterized by a Mediterranean climate having cool and wet winters and hot and dry summers. The dry season usually starts in Jun and continues until the middle of October but the temperature increases from north to south of the basin, with large intra-annual variability. In total, the average annual precipitation ranges between 150 mm in the south (arid part) and 7500 mm in the north (semiarid part) KRB (Muthuwatta et al., 2010). The multipurpose KR, with a designed storage capacity of 7.5×10^9 m^3 and live storage capacity of 4.7×10^9 m^3, is located in the northwestern province of Khuzestan and became operational in August 2002 (Fereidoon and Koch, 2017). The objectives of the dam are providing the water for irrigation of 320,000 ha of the agricultural lands in the Khuzestan plains, i.e. the lower sections of the KRB, as well as hydroelectric power generation, amounting to 934 GWh per year, and, not to the least, flood control in the agriculturally used lands in the downstream sections of the river basin.

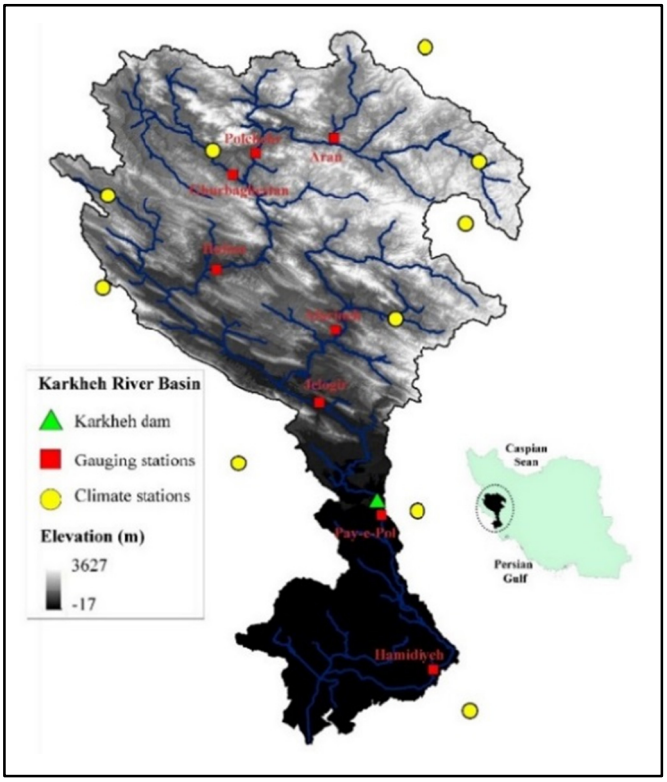

Fig. 1. Map of the Karkheh River Basin with weather stations and the Karkheh dam.

3. Material and methods

3.1. Data

The hydroclimate data consists of daily precipitation- and max/min air temperature time series from 10 climate stations, as well as outflow data from the KR and streamflow records at 8 gauging stations, depicted in Fig. 1, for a period of 1982–2004 (Fereidoon and Koch, 2017). The SWAT model uses a digital elevation model (DEM) map at a resolution of 90 m (NASA) to delineate the watershed and to extract the stream network in the KRB.

Land-use maps with a resolution of 900 m were obtained from Mahab Ghods Engineering company and soil data further required in SWAT from FAO (1995) for two depth layers (0–30 cm and 30–100 cm depth) at a spatial resolution of 10 km. Technical specifications of the KR, such as maximum and minimum storage capacity, net evaporation rates and height-area-volume curves in the reservoir, were obtained from Iran Water and Power Resources Development (IWPCO). The percentile areas devoted presently to the different crops in five the main agricultural sectors south of the KR, as well as their growth periods, are listed in Table 1.

3.2. Simulation and optimization models

3.2.1. Hydrological model SWAT

SWAT is a semi-distributed and basin-scale water-balance hydrological model that is able to simulate flow and transport through the land-phase of the hydrological cycle in large and complex watersheds with varying soils, land use and management conditions (Arnold et al., 1998; Neitsch et al., 2002). SWAT has by now found countless applications all across the world (see Gassman et al., 2014, for a review) related to such varied hydrological issues, such as the classical prediction of streamflow, but also the estimation of the impact of land management practices on sediment erosion and nutrient cycling (Ullrich and Volk, 2009). In recent years the SWAT-analyses of the impacts of climate change and/or changing land-use practices on streamflow and water yield are coming more to the fore (Varanou et al., 2002; Koch and Cherie, 2013; Kundu et al., 2017).

In SWAT the spatial variability in a basin is represented by dividing the total basin into sub-basins (=198 in the present basin) which are then, based on the topography (DEM), soil type, land-use and,

Table 1
Percentile distribution of present crops in five agricultural plains, Dasht-e Abbas (DA), Dosalegh (DO), Arayez (AR), Hamidiyeh (HA) and Azadegan (AZ), downstream of the KR and growth periods of crops.

Crop	DA	DO	AR	HA	AZ	Growth period
Winter wheat	21	16.6	23.3	21.6	23.1[a]	November–June
Barley	12.2	13.1	13.3	12.5	13.8[a]	November–June
Maize	8.9	9.6	10.7	9.1	9.7[a]	June–October
Broad beans	1.9	2.2	2.1	4.3	3.3	June–October
Green beans	0	4.4	3.6	0	0	July–October
Sesame seed	3.1	0	0	0	0	June–October
Cucumbers	4.7	13.1	11.7	7.4	5.5	February–June
Tomatoes	2.7	4	6	5	3.7	September–December
Watermelons	4.1	7.3	6.9	5.5	4	March–June
Alfalfa	18.8	19.3	16.2	10.7	8.4	November–April
Sorghum	4.1	0	0	6.1	4.6	February–May
Sugarcane	3.5	5.3	0	0	0	June–October
Rapeseed	1.6	2.2	3.4	4.5	3.5	June–October
Eggplants	4.2	0	0	8.8	6.4	May–September
Citrus	9.4	0	0	0	0	Whole year
Carrots	0	3	2.7	4.5	3.5	November–June
Dates	0	0	0	0	10.5	Whole year

[a] These data were missing in the reference report and collected from other references.

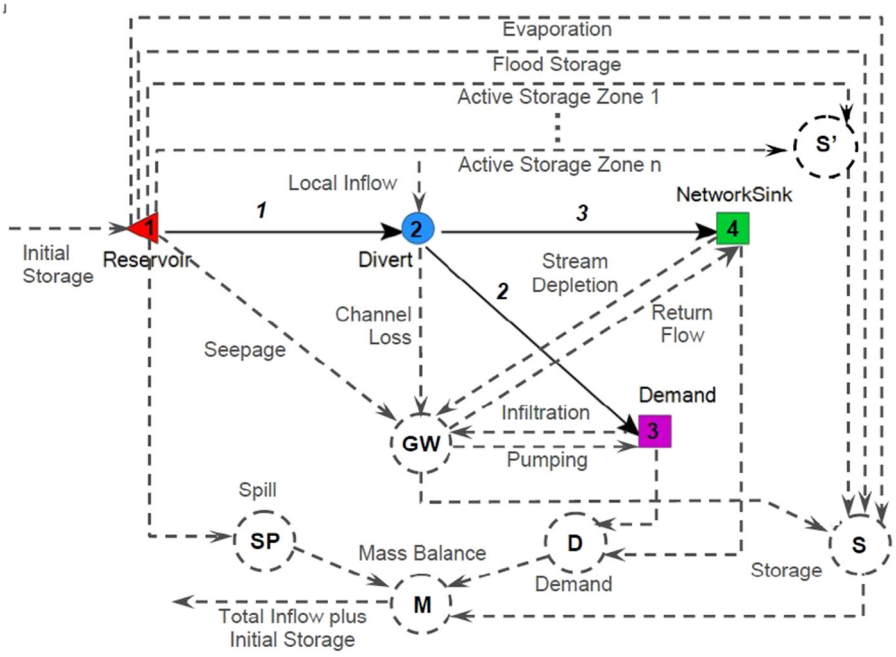

Fig. 2. MODSIM network structure with artificial nodes and links (after Labadie, 1995).

optionally, slope characteristics, further subdivided into so-called hydrologic response units (HRUs) with identical characteristic of some of these properties. For the present large and complex KRB, the total number of HRU's amounts to >11,000. After the GIS-setup of the model (see Fereidoon and Koch, 2016, 2017; for details), SWAT then simulates - by solving the water balance equations incrementally on a daily time step - the various hydrological processes by routing the driving precipitation, (plus snowmelt minus the evapotranspiration) through the surface and shallow subsurface compartments of the hydrological cycle towards the collecting streams.

Despite its overall good conceptual description the land-phase of the hydrological cycle, SWAT still requires the adjustment or calibration of a large number of "tweaking" parameters. Historically, the classical approaches in SWAT have been trial and error calibration and/or the deterministic Parameter Solution (ParaSol) automatic method (e.g. Koch and Cherie, 2013). Nowadays, the most commonly used calibration method in SWAT appears to the stochastic Sequential Uncertainty Fitting 2 (SUFI-2, version 2) embedded within SWAT-CUP (Calibration and Uncertainty Program) (Abbaspour et al., 2004). It has also been used here. SUFI quantifies the uncertainty of a calibrated parameter by the 95% prediction uncertainty band (95PPU) calculated at the 2.5% and 97.5% levels of the cumulative distribution function obtained through Latin hypercube sampling of the output objective function, i.e. the cumulative squared misfit between observed and simulated streamflow values.

The performance of the final calibration model is then evaluated by two indices: P-factor and R-factor. The P-factor is the percentage of measured data covered by the 95 PPU band. Its value ranges between 0 and 1. For river outflow, a value of $P > 0.7$ has been reported to be satisfactory (Abbaspour et al., 2007). The R-factor denotes the relative width of the 95 PPU band divided by the standard deviation of the measured variable. It ranges between 0 and infinity and a value < 1 is stated to be desirable for a parameter (Moriasi et al., 2007). The quality of the fit of the model output, namely, streamflow, to the observed one is measured by the RMSE, the R^2, and the Nash–Sutcliff efficiency (NSE) (Abbaspour et al., 2004).

3.2.2. Water allocation model MODSIM

The MODSIM river basin network model is a river basin management decision support system (DSS) model for the analysis of long term operational planning and short term water management, drought contingency planning and for resolving conflicts between urban, agricultural and environmentally concerned stakeholders (Labadie, 1995). Although the model has been used for the simulation of river systems worldwide (Larson and Spinazola, 2000; Marques et al., 2006; Sulis and Sechi, 2013), it appears to be not so well-known.

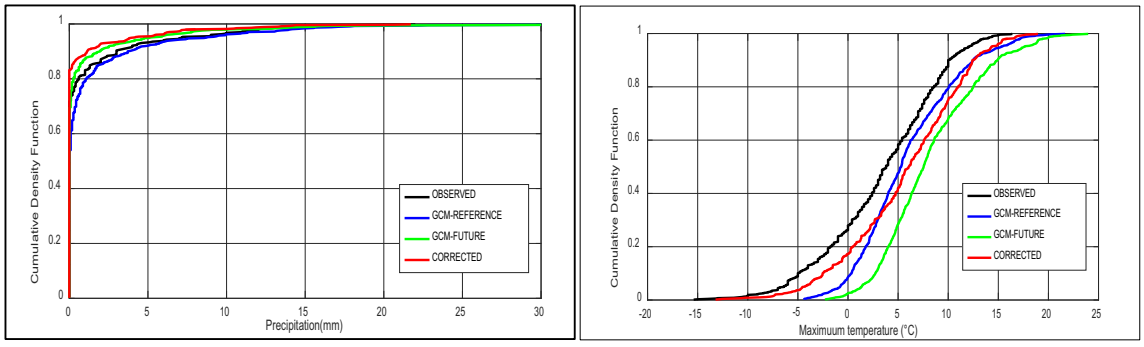

Fig. 3. ECDFs of daily precipitation (left) and maximum temperature (right) in 15th January at a weather station for observed (1982–2004), reference GCM and future (2038–2060) GCM and bias-corrected data for RCP4.5 scenario.

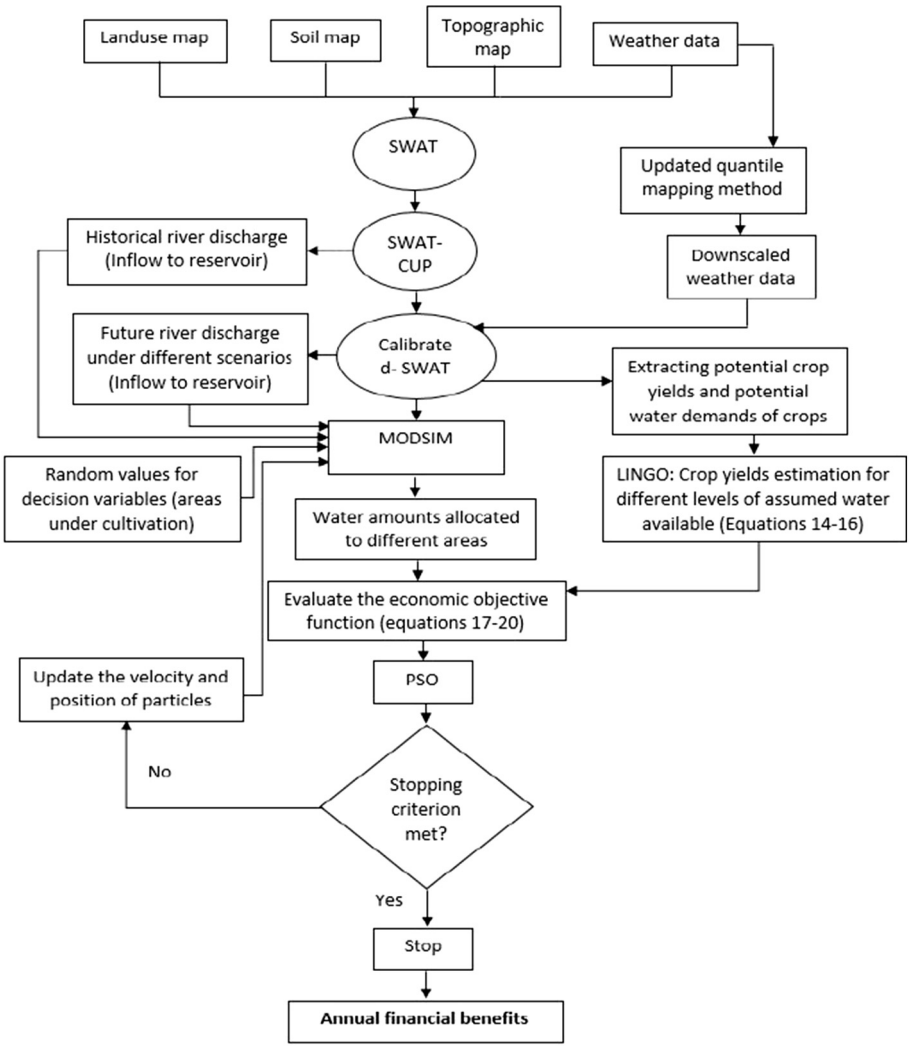

Fig. 4. Flowchart of the iterative simulation-optimization model for maximization of agricultural benefits.

MODSIM uses a state-of-the-art network flow optimization (NFO) algorithm to allocate flows in a river basin, in accordance with specified water rights and other priority rankings (Labadie, 1995). The complete scheme of the MODSIM network is shown in Fig. 2. Once the links and nodes are defined by users (solid lines), some accounting artificial nodes and links (dashed line) are created automatically to satisfy the mass balance throughout the entire MODSIM network.

The extracted historic and future river flow to the KR, as simulated with the SWAT model for different scenarios, enters the network and is allocated to the agricultural areas (demand nodes), such that the costs over a given planning time period are minimized. Thus, the following linear optimization problem is solved by MODSIM:

$$\text{Minimize} \qquad \sum_{k \in A} c_k q_k \tag{1}$$

subject to:

$$\sum_{k \in O_i} q_k - \sum_{j \in I_i} q_j = 0; \quad \textit{for all nodes } i \in N \tag{2}$$

$$l_k \le q_k \le u_k; \quad \textit{for all links } k \in A \tag{3}$$

Table 3
Initial and final ranges of the 7 most sensitive SWAT calibration parameters.

Parameter name	Definition	Initial range	Final range
r__CN2	SCS runoff curve number	−0.4 to 0.4	−0.32 to −0.16
v__GWQMN	Threshold depth of water in shallow aquifer required for return flow	1500 to 3500	1520 to 2538
v__ALPHA_BF	Base flow alpha factor	0.4 to 1	0.56 to 0.87
v__EPCO	Plant uptake compensation factor	0.2 to 0.7	0.27 to 0.55
r__SOL_BD	Moist bulk density	0 to 0.35	0 to 0.23
v__RCHRG_DP	Deep aquifer percolation fraction	0.1 to 0.7	0.25 to 0.64
v__SHALLST	Initial depth of water in shallow aquifer	2500 to 4000	2930 to 3849

Table 4
Statistical measures for monthly outflows at the 8 gauging stations for calibration and validation periods.

Station	P-factor	R-factor	R^2	NSE
	cal/val	cal/val	cal/val	cal/val
Aran	0.76/0.78	1.18/1.09	0.62/0.61	0.59/0.56
Polchehr	0.81/0.85	1.19/1.03	0.68/0.64	0.52/0.63
Ghurbaghestan	0.88/0.88	1.37/1.05	0.61/0.81	0.54/0.80
Hulian	0.70/0.73	0.97/0.77	0.77/0.76	0.73/0.74
Afarineh	0.94/0.88	1.26/0.82	0.70/0.69	0.62/0.52
Jelogir	0.78/0.82	1.09/0.87	0.83/0.81	0.82/0.80
Pay-e-Pol[a]	0.72/0.88	1.00/1.08	0.78/0.68	0.78/0.66
Hamidiyeh[a]	0.65/0.66	1.21/0.98	0.79/0.65	0.72/0.61

[a] Stations located downstream of the Karkheh dam.

where A is the set of all arcs or links in the network; N is the set of all nodes; Oi is the set of all links originating at node i (i.e. outflow links); Ii is the set of all links terminating at node i (i.e. inflow links); qk is the integer valued flow rate in link k; ck are cost weighting factors, or water right priorities per unit flow rate in link k, that are computed by Eq. (4); and lk and uk are lower and upper bounds, respectively, on the flow in link k.

The cost factor ck in Eq. (4) encompasses both storage right and stakeholder demand priorities in link k and is written for the former (reservoir) as

$$c_k = -(50,000 - 10 * OPRR_k) \tag{4}$$

and for the later (demands) as

$$c_k = -(50,000 - 10 * DEMR_k) \tag{5}$$

where $OPRR_k$, and $DEMR_k$ are chosen integer priority rankings between 1 and 5000 for the reservoir and the demands, respectively, with lower numbers indicating a higher ranking, i.e. more negative cost. With this notation in Eqs. (4) and (5), the minimization of negative costs in Eq. (1) is equivalent to maximizing flows to the higher ranked water uses. The cost factor of Eq. (4) represents the costs of carryover- and changing storage in the reservoir and depends on the local reservoir operation policy. As the latter is not exactly known for the KR-dam, the simplest one named standard operation policy (SOP), which aims to release as much water as is demanded (computed by the demand nodes in MODSIM), storing only surplus water for the next month, is used here. To do this, a high priority number (low priority) is given to the reservoir node/link.

The number of demand cost factors in Eq. (5) is k = 22, consisting of 5 agricultural regions * 4 crops (wheat, barley, maize, other crops) = 20 agricultural links, plus 1 municipal link, plus 1 environmental link of minimum water. It should be noted that, as there is not real priority of one region/crop over the other one, all their priority ranking numbers are set equal. Eqs. (1)–(3) are solved with the efficient Lagrangian relaxation algorithm based on a dual coordinate ascent, called RELAX-IV (Bertsekas and Tseng, 1994).

3.2.3. Stretched particle swarm optimization (SPSO)

Particle swarm optimization (PSO) is a robust stochastic evolutionary optimization technique proposed by Eberhart and Kennedy (1995). PSO is based on the movement and intelligence of swarms that can be used to find approximate solutions to extremely difficult maximization and minimization problems which can have multiple local maxima/minima in an iterative process, i.e. as a global optimization method it overcomes many of the problems adherent to classical gradient methods, namely, the trapping of a solution in a local minimum. An extension of the classical PSO which is better in finding global solutions of "multi-valley" objective functions is the stretched PSO (SPSO), (Parsopoulos and Vrahatis, 2002).

Assuming a D-dimensional search space of the objective function, with D is the number of decision variables, classical PSO starts with a (best) position of the i-th particle of the swarm, $P_i = (p_{i1}, p_{i2}, \ldots, p_{iD})$ and moving then to a new location $X_i = (x_{i1}, x_{i2}, \ldots, x_{iD})$ with the velocity $V_i = (v_{i1}, v_{i2}, \ldots, v_{iD})$, using the prescriptions of Eqs. (6) to (9) (Eberhart and Shi, 1998):

$$v_{id}^{n+1} = \chi\left(\omega^n v_{id}^n + c_1 r_1^n \left(p_{id}^n - x_{id}^n\right) + c_2 r_2^n \left(p_{gd}^n - x_{id}^n\right)\right) \tag{6}$$

$$x_{id}^{n+1} = x_{id}^n + v_{id}^{n+1} \tag{7}$$

$$\omega^n = \frac{\left(\omega^{max} - \omega^{min}\right) \times n}{n_{max}} \tag{8}$$

$$v^{min} \le v_{id} \le v^{max} \tag{9}$$

where $d = 1, \ldots, D$, g defines the index of the best particle in the swarm, and superscript n denote the iteration number, where ω is called inertia weight which is changing during the iteration, c_1, c_2 are two positive real numbers, called cognitive and social weights, respectively and χ is a constriction factor (used in this already extended version of the PSO), which is employed, alternatively to ω, to limit the velocity to the range $[v^{min}, v^{max}]$.

As mentioned above, to avoid possible trapping of swarm particles in some local minima and so to improve the convergence of the PSO to a, hopeful, global minimum, an extension of the method by including a function stretching technique (SPSO) was proposed by Parsopoulos and Vrahatis (2002). The idea behind SPSO is to use a two-stage transformation of the original objective function $f(x)$ in the form:

$$G(x) = f(x) + \gamma_1 \|x - \bar{x}\| (\, sign(f(x) - f(\bar{x})) + 1) \tag{10}$$

$$H(x) = G(x) + \gamma_2 \frac{sign(f(x) - f(\bar{x})) + 1}{tanh(\mu(G(x) - G(\bar{x})))} \tag{11}$$

where γ1, γ2, and μ are user-defined parameters, and $\bar{x}$ is a local

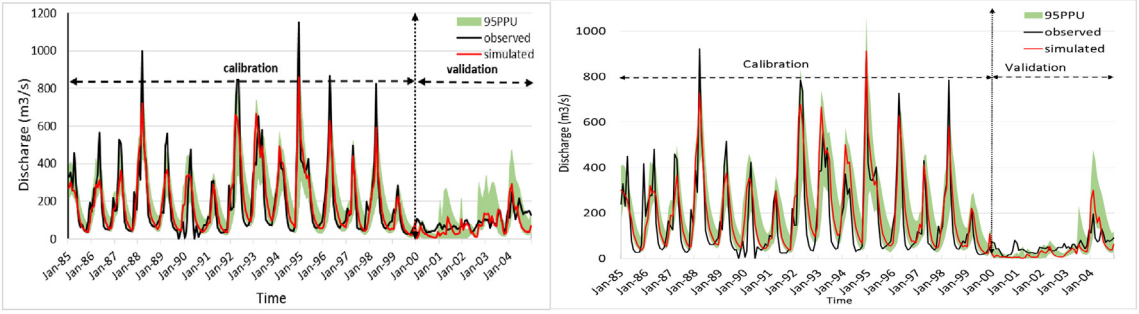

Fig. 5. Observed and simulated monthly outflow (m^3/s) for calibration and validation at Pay-e-Pol (left) and Hamidiyeh (right) stations.

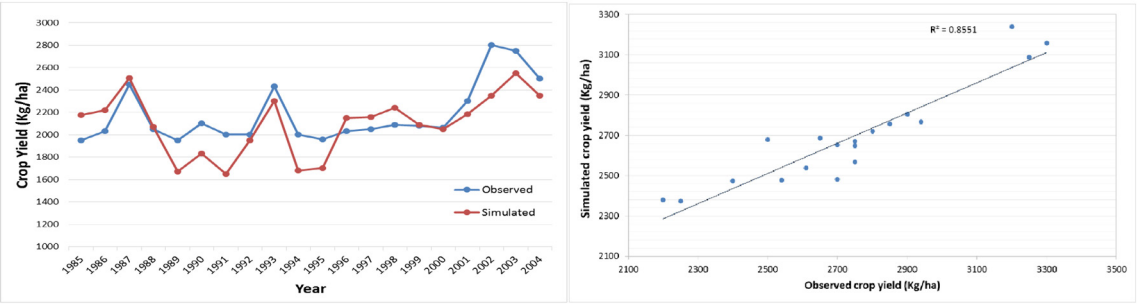

Fig. 6. Observed and simulated annual winter wheat yields (left panel) and plot of simulated over observed annual values with linear regression line (right panel) for the DA plain for the reference period (1985–2004).

minimum. Basically, the first transformation stage, G(x) of Eq. (10), elevates the function f(x) and, so, eliminates most of the local minima, while the second one, H(x) in Eq. (11) stretches the neighborhood of x upwards, since it assigns higher function values to those points.

The SPSO-algorithm prescribed in its most rudimentary form by Eqs. (6)–(11) has been programmed in the MATLAB© - environment to solve the constrained maximization problem, Eqs. (1)–(3), wherefore maximizing a function is equivalent to minimizing its negative, i.e. the objective function, Eq. (1), is multiplied by −1, before the SPSO is applied.

3.3. Downscaling of GCM-climate predictors

In this study, future predictions of the HadGEM2-ES climate model have been adopted for downscaling and error correction. The HadGEM2-ES is an earth system model developed by the Hadley Centre (Collins et al., 2011) with a horizontal solution of 1.875° × 1.275° and 38 vertical levels for the atmosphere and of 1° (increasing to 1/3° at the equator) with 40 levels for the oceans (Betts et al., 2015). HadGEM2-ES has been used up-to-date for future climate change simulations under various representative concentration pathways (RCPs) (Jones et al., 2009; Caesar et al., 2013). In the present study, HadGEM2-ES-predictors with RCP4.5 and RCP8.5, corresponding to moderate and high greenhouse gas emissions, with atmospheric radiative forcings of 4.5 and 8.5 W m^{-2} by year 2100, respectively (Taylor et al., 2012), are used for further downscaling.

For downscaling a bias-correction (BC) technique (e.g. Teutschbein and Seibert, 2012) has been used which appears to overcome some of the deficiencies of classical statistical downscaling methods (Koch and Cherie, 2013; Wilby and Dawson, 2013), namely, for the prediction of precipitation. The basic idea of a BC-method is to either use some power transformation and/or distribution mapping of the GCM-predictors so that some statistical characteristics, such as mean and variance agree with those of the observed time series.

A particular powerful BC-method which corrects the entire distribution of the predicted time series and, so better reflects the whole variability of the observed series, is quantile mapping (QM) (Wood et al., 2004; Maurer, 2010; Themeßl et al., 2012) and it is used in the present study. More specifically, QM is applied to the GCM-raw outputs (max/min temperature and precipitation) on a daily basis to correct their bias against the observed data in each grid cell using the empirical cumulative density distribution function (ECDF) for each calendar date of the year. For example, taking a particular day, say January 15th, and using a sliding window of 31 days in the 14-year of calibration time period, all daily precipitation observations are lumped together in one basket to create a distribution of daily precipitation observations for January 15th of n = 14 × 31 = 434 days.

The first step in the QM-method consists in estimating the *ECDFs* for a given probability P_d of both the observed $X_d^{obs,\,ref}$ and the GCM-simulated climate data $X_d^{GCM,\,ref}$ in the reference period and computing the difference

$$CF_d^{GCM,ref} = ECDF_d^{obs^{-1}}\left(P_d^{GCM,ref}\right) - ECDF_d^{GCM,ref^{-1}}\left(P_d^{GCM,ref}\right) \quad (12)$$

of the two inverse *ECDFs*.

The corrected time series $Y_d^{cor,\,fut}$ for the future period is then obtained by adding the correction term $CF_d^{GCM,\,ref}$ to the raw future GCM value $X_d^{GCM,\,fut}$:

$$Y_d^{cor,fut} = X_d^{GCM,fut} + CF_d^{GCM,fut} \quad (13)$$

where, for simplicity, it is assumed that the future correction term $CF_d^{GCM,\,fut} = CF_d^{GCM,\,ref}$ applies also for the future prediction period. It should be noted that for the bias correction of the precipitation data Themeßl et al. (2012) advocated a so-called frequency adaption (FA), to be applied when the empirical frequency of the simulated dry days is greater than that of the observed ones. While FA has also been implemented here, it was turned on, as the frequency of the GMC - predicted dry days concurred reasonably well with the observed one.

For a better understanding of the working mechanism of QM method, the bias-corrected precipitation (left) and maximum temperature (right) of 15th January for the future period 2038–2060 at a weather station in the northeast of the KRB predicted for the RCP4.5 scenario is shown in Fig. 3. On may notice that the reference GCM-predictions for both the precipitation and the max temperature systematically overestimate the corresponding observed ones, so that the biased correction terms are negative in both situations.

3.4. SWAT – estimation of crop yields and water requirement

3.4.1. Crop yield estimation

Prior to the MODSIM simulation/optimization of the optimal water allocation for the agricultural areas in the KRB with its crop distribution as defined in Table 1, the corresponding crop yields are estimated by

Table 5
Monthly efficiency coefficients of the adjustments to the observed data before (Raw) and after QM-bias correction (BC) for calibration and verification periods.

Efficiency coefficient	Rainfall		Max temp		Min temp	
	Raw_GCM	BC_GCM	Raw_GCM	BC_GCM	Raw_GCM	BC_GCM
Calibration period (1982–1995)						
R^2	0.72	0.85	0.89	0.91	0.88	0.91
NSE	0.63	0.68	0.72	0.88	0.75	0.92
IA	0.89	0.96	0.96	0.99	0.93	0.99
Verification period (1996–2004)						
R^2	0.68	0.83	0.88	0.91	0.89	0.93
NSE	0.61	0.68	0.77	0.96	0.72	0.95
IA	0.88	0.93	0.96	0.98	0.95	0.99

Table 6
Relative changes in precipitation (%) and mean air temperature (°C) for the future scenarios.

Subbasin	Precipitation				Mean temperature			
	RCP 4.5 (2038–2060)	RCP 4.5 (2078–2100)	RCP 8.5 (2038–2060)	RCP 8.5 (2078–2100)	RCP 4.5 (2038–2060)	RCP 4.5 (2078–2100)	RCP 8.5 (2038–2060)	RCP 8.5 (2078–2100)
Qarasou	+8%	−3%	−1%	+14%	+1.6	+1.8	+1.8	+3.3
Gamasiab	+7%	−2%	−9%	+12%	+0.2	+1	+1	+1.5
Seymareh	+4%	−4%	−6%	+8%	+1.8	+2.1	+2.1	+3.2
Kashkan	+11%	+0.5%	−8%	+20%	+0.2	0	0	+1.2
South Karkheh	+23%	+14%	+6%	+31%	+1	+1.8	+1.1	+3.2

SWAT for each HRU (Baumgart, 2005). The sensitive crop parameters required for the crop yield module of SWAT are collected from Vaghefi et al. (2014).

3.4.2. Crop water requirement

In order to allocate the appropriate amount of irrigation water to each crop, it is necessary to know how much water a plant needs per month. To that avail the "Auto-irrigation initialization from unlimited source outside watershed" in the SWAT-model is employed. According to this option, any time the actual plant growth falls below the water stress threshold the model will automatically apply water to the associated HRU. The crop yield water needs are computed with the calibrated SWAT model for the baseline period and the future scenarios and then used in the MODSIM model.

3.5. MODSIM-LINGO-PSO maximization of the annual agricultural benefit

3.5.1. Overview and flow chart of the 3-stage procedure

The ultimate goal of the present study is the maximization of the annual benefits from multi-crop irrigation areas in the KRB. Actually this is an iterative three-stage process. In the first stage the classical MODSIM approach, employing the SWAT-simulated monthly inflow to the Karkheh-reservoir (see Fig. 2), solves the constrained optimization problem, Eqs. (1)–(3), for getting the optimal water allocation to different water users under the pre-specified priority constraints. Stages two and three, discussed below, involve then the application of LINGO linear programing to maximize the crop yields in response to different levels of assumed water availability and finally, the maximization of the annual economic agricultural benefits with PSO, respectively. The iterative optimization scheme is stopped when no more significant improvements in the objective function are obtained. Fig. 4 shows the flow chart of the iterative procedure with the intertwined three stages, with stages two and three explained in detail in the following paragraphs.

3.5.2. LINGO-maximization of crop yields

The idea behind the maximization of the crop yields is that in a semi-arid region like the KRB, there is not sufficient water to fully satisfy the crop water requirements, i.e. deficit irrigation is applied. Similar to Banihabib et al. (2016), the FAO-accepted crop yield response to deficit irrigation (Stewart and Robert, 1973) is considered as objective function (Eq. (14)), constrained by the range of allocated water to each crop (Eq. (15)), as computed by MODSIM (see Fig. 4), and the total potential water amount of the crop (Eq. (16)), i.e.

$$\text{Maximize} \qquad Y_c^a/Y_c^{max} = 1-\sum_{i=1}^{g} k_{i,c}^{y}\left(1-w_{i,c}^{a}/w_{i,c}^{p}\right) \tag{14}$$

subject to

$$0 \le w_{i,c}^{a} \le w_{i,c}^{p} \tag{15}$$

$$\sum_{i=1}^{g} w_{i,c}^{a} \le X W_c^p \tag{16}$$

where X = 1.0, 0.95., 0.9, …, until Y_c^a becomes 0; Y_c^a = actual crop yield (ton/ha); Y_c^{max} = potential crop yield (ton/ha); $w_{i,c}^{a}$ = allocated water to crop c in growth stage i (m^3/ha); $w_{i,c}^{p}$ = potential water demand of crop c in stage i (m^3/ha); $k_{i,c}^{y}$ = crop yield response factor to water deficit of

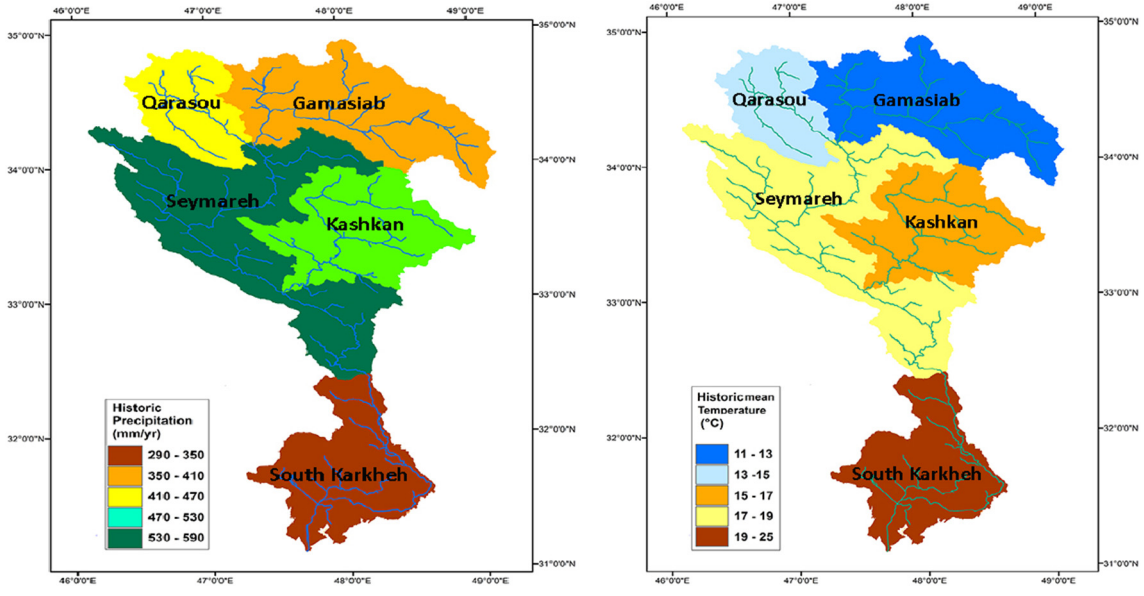

Fig. 7. Distribution of average annual precipitation (left panel) and mean annual temperature (right panel) for the historic period (1982–2004) in the five sub-basins of the KRB.

crop c in stage i; and W_c^p = total potential water demand of crop c over all growth stages (m^3/ha). The crop yield response values $k_{i,c}^y$ at the different growth stages ($i = 1, \ldots, g$) of the crop development are collected from a FAO-report "Yield Response to Water" (Doorenbos and Kassam, 1979). Potential crop yields Y_c^{max} and potential water demands W_c^p are determined by the SWAT "auto-irrigation initialization from unlimited source outside watershed"–module, as mentioned in the previous section. It means essentially that the yield of a crop will be maximal, when its total water requirement is completely fulfilled by irrigation. Eqs. (14)–(16) are solved by means of the LINGO-linear programing package.

3.5.3. PSO-maximization of economic agricultural benefit

In the third stage the average annual economic benefit of using a particular multi-crop pattern in the KRB, with the optimal yield for each crop determined in the second stage under deficit water availability determined in the first stage (see Fig. 4), are maximized. The optimal amount of water allocation which depends on the areas under cultivation in a multi-crop model specifies the available water use among several crops, such that the annual profit from all crops in the agricultural areas is maximized.

The (linear) objective (cost) function and constraints are expressed as follows:

$$\text{Maximize} \qquad B_{ann} = \frac{1}{n}\left(\sum_{i=1}^{n}\sum_{c=1}^{k} P_i^c \times Y_i^c \times A_i^c\right) \tag{17}$$

subject to:

$$S_{t+1} = S_t + I_t - R_t - EV_t \tag{18}$$

$$S_{min} \le S_t \le S_{max} \tag{19}$$

$$A_{min}^c \le A_i^c \le A_{max}^c \tag{20}$$

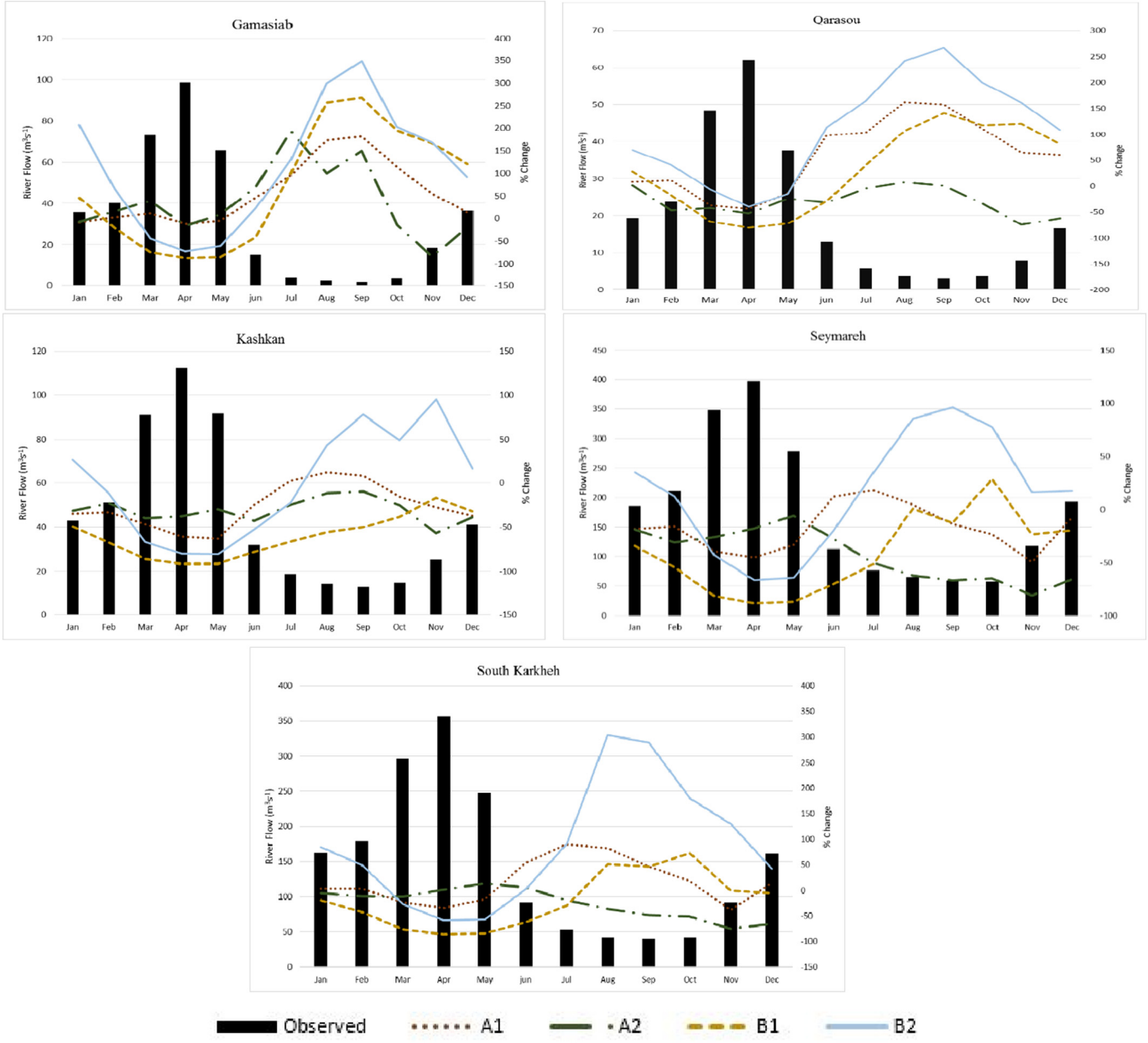

Fig. 8. Average monthly river discharge ($m^3\ s^{-1}$) of the Karkheh river for the historical and the future scenarios/periods for five KRB-sub-basins. Notations are: A1 = RCP 4.5/2038–2060, B1 = RCP 8.5/2038–2060, A2 = RCP 4.5/2078–2100, B2 = RCP 8.5/2078–2100.

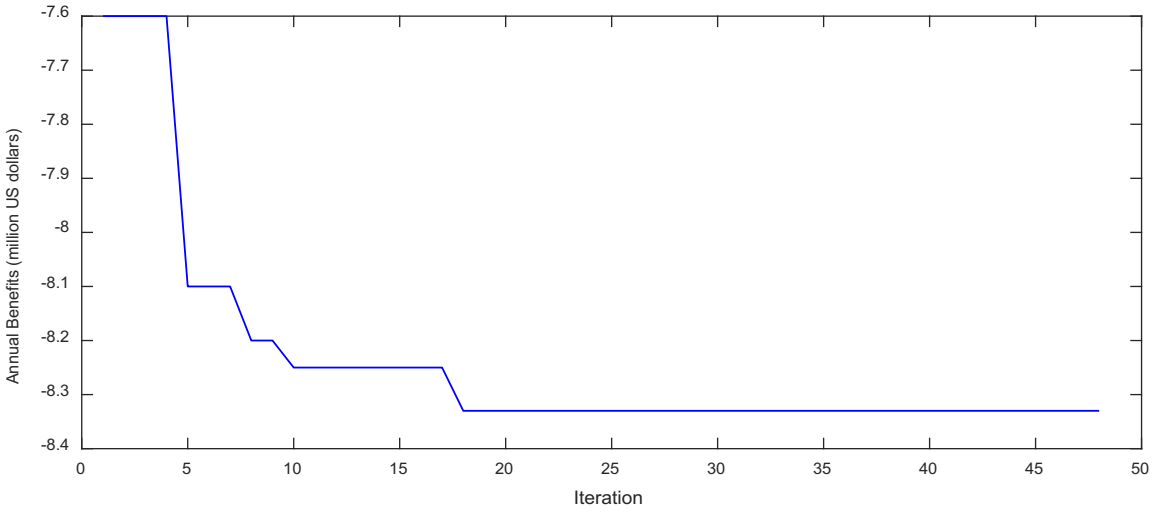

Fig. 9. Annual benefits as a function of iteration in the PSO procedure for RCP 4.5/2038–2060 scenario/period.

where B_{ann} = annual benefit; P^c = unit benefit (price) of crop c (rials kg^{-1}); Y^c = crop yield (kg ha^{-1}); A^c = area under crop cultivation (ha); n = number of years of the planning horizon; c = type of crop; i = year of cultivation; k = number of agriculture crop productions; t = monthly time step; S = storage capacity of reservoir; I = stream flow; R = reservoir outflow; EV = volume of reservoir evaporation. Eqs. (17)–(20) are solved by PSO, wherefore the following prices P of three major crops the Iranian government pays to the farmers are used in Eq. (16): Wheat: 12705 rials kg^{-1}, maize: 10368 rials kg^{-1} and barley: 10028 rials kg^{-1}. To convert to US$ one may divide these numbers by 40,000 rial/US$.

For simplicity and lack of other information, these prices are also assumed in the near future (2038–2060) scenarios. It should be noted that the annual benefit B_{ann} is in fact the revenue, not the net income or

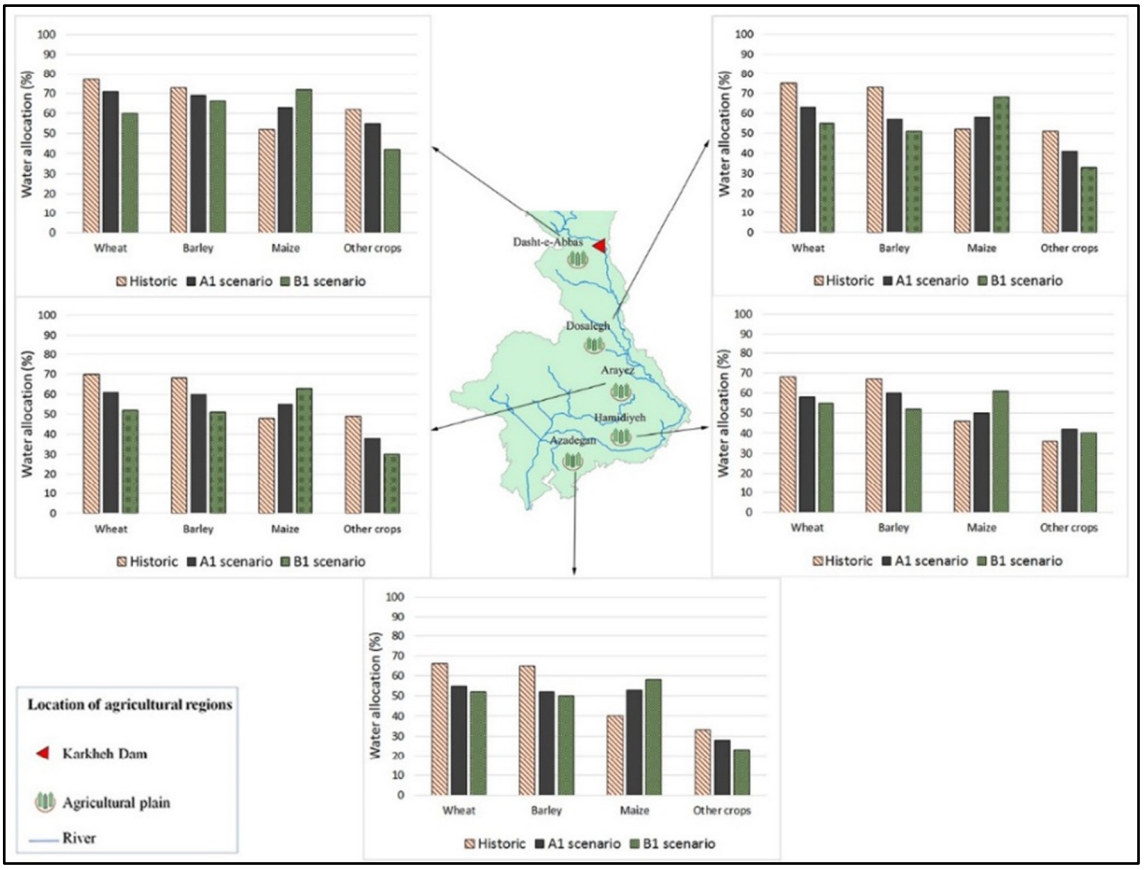

Fig. 10. Percentage of water allocation in 5 main agricultural regions of the KRB for different crops and three scenarios/periods: Historic, A1 = RCP 4.5/2038–2060 and B1 = RCP 8.5/2038–2060.

profit, as it does not include the costs the farmers incur for the crop production itself. These costs are highly varied, because of the unknown labor costs, unknown amounts of fertilizers applied and inflation. However, as these costs are more or less the same for the three cereal crops, they would act only as a negative constant in Eq. (17), i.e. should not affect much the outcome for the optimized decision variables, other than reducing the net income. Besides, because of the inevitable uncertainties in the projected scenarios, such as land use changes, inflation and population growth, the model is analyzed only for the baseline (reference) period and the near-future (2038–2060) period.

3.6. Practical implementation of the SLMP-model

The practical implementation of the coupled SMLP-model - following the flow chart of Fig. 4 and the explanations of the previous sections - starts by SWAT-determination of the inflow into the KR under historic and future climate scenarios. The inflow time series are then entered into MODSIM to allocate water to the different agricultural regions under the given priority weights. At the same time, the potential crop yields and the associated potential water demands for each crop are determined with SWAT, with these values being further used to optimize the actual crop yield (under deficit irrigation), using LINGO linear programing. Multiplying the latter by the area under cultivation, the total water requirement for this crop is obtained, which is then defined as a demand node value in the MODSIM customization module. The different crop cultivation areas are then the decision variables in the final, iterative MODSIM-PSO process to optimally allocate water among the different cultivation areas, such that the total agricultural economic profits over the planning time horizons become maximum.

4. Results and discussion

4.1. SWAT-calibration, validation and sensitivity analysis of streamflow discharge

To evaluate the SWAT-model's performance, the SUFI-2 algorithm included in the SWAT-CUP software package was used. Calibration, validation and sensitivity analysis was performed on measured stream flows from 8 gauge stations for the 1985–1999 and 2000–2004 time periods, respectively, wherefore three years (1982–1984) were considered for model warm up. Seven parameters were identified as sensitive in this study (see Table 3) in all sub-basins, but with different ranks of sensitivity. For example, groundwater and soil parameters were found to be most sensitive in lowland catchments, while runoff parameters are the most sensitive ones in mountainous or low mountain range catchments (Schmalz and Fohrer, 2009). This is because under areas with lower slopes rainfall infiltration accumulates more, leading to higher groundwater levels and, subsequently, to more baseflow. Hence, groundwater parameters, GWQMN, ALPHA_BF, RCHRG_DP and SHALLST, followed by soil parameter SOL_BD were identified to be more sensitive in the low-elevation (southern) parts of the KRB than in the northern part of the KRB with higher elevations. It should be noted that the Curve Number at moisture condition II (CN2) was found to be the most sensitive parameter for the catchment as a whole.

SWAT-model's performance results as evaluated by the four statistical measures, P-factor, R-factor, R^2, NSE for the prediction of the monthly streamflow at the eight outlets are listed in Table 4 for both calibration and validation periods and indicate, according to the classification of Moriasi et al. (2007), that the simulated streamflows are all in

Fig. 11. Comparison of MODSIM-PSO computed optimal allocated crop area values for three scenarios/periods: historic, A1 = RCP 4.5/2038–2060 and B1 = RCP 8.5/2038–2060.

Table 7
Optimal crop areas (hectare) computed by the SLMP–model for the three scenarios/periods in comparison with the actual historic, authorities-projected future maximum and minimum crop cultivation areas.

Agricultural plain	Crop	Max	Min	Actual historic	Historic SLMP	RCP 4.5/2038–2060 SLMP	RCP 8.5/2038–2060 SLMP
DA	Winter wheat	4710	2210	3995	4710	3244	2303
	Barley	2730	1480	2321	2253	1520	1480
	Maize	1985	735	1693	1009	1985	1985
	Other crops	12,970	10,470	11,015	12,320	11,872	11,860
DO	Winter wheat	3300	2050	2678	3300	3225	2050
	Barley	2600	1350	2113	2210	1767	1730
	Maize	1900	650	1549	812	1737	1983
	Other crops	12,050	9550	10,800	11,970	11,723	11,374
AR	Winter wheat	6280	3780	5592	5242	4880	4280
	Barley	3590	2340	3192	3190	2892	2590
	Maize	2900	650	2568	910	1150	1443
	Other crops	14,230	11,730	12,648	12,298	12,098	11,950
HA	Winter wheat	4665	2165	3683	3778	3080	2403
	Barley	2700	1450	2131	2102	1888	1710
	Maize	1965	715	1551	910	1150	1443
	Other crops	12,300	9800	11,023	10,944	9930	9750
AZ	Winter wheat	15,000	11,250	14,280	13,756	11,872	11,370
	Barley	9100	6600	7140	7880	6944	6600
	Maize	6400	3900	5100	3900	3970	4210
	Other crops	34,800	31,050	33,480	32,071	31,133	31,050

either “satisfactory”, “good” and “very good” ranges. The last two stations in Table 4, Pay-e-Pol and Hamidiyeh, are located downstream of the Karkheh dam, so that their measured streamflows are strongly affected by the dam's operational rules. Fig. 5 shows that the monthly observed outflows at these two station are well fitted for the calibration period (1985–1999), but less so for the validation period (2000–2004). In fact, as the Karkheh dam started its operation in August 2002, its impact on the streamflow, i.e. a tremendous decrease of >50% of the average annual streamflows in the two subsequent years 2003–2004, is clearly noticeable, namely, for some months after the Karkheh dam became operational, in the time of which the SWAT's reservoir module characteristic were not well documented (Fereidoon and Koch, 2016).

4.2. Crop yield assessment

Using the appropriate ranges of crop parameters collected from different references (i.e. Baumgart, 2005; Vaghefi et al., 2015) in the SWAT model, the annual crop yields for the various crops are evaluated. Fortunately, SWAT appears to be able to do this in a satisfactory manner without a detailed calibration, given the lack of long-term observed crop yield data in the study region (Srinivasan et al., 2010), namely, for the non-cereal crops, which are available just for a few years. In these situations, the standard SWAT crop parameter values are used to determine the average annual crop yield to be as closely as possible to the average observed one. Fig. 6 (left) shows the observed and simulated annual winter wheat yield series for the DA plain for the reference period (1985–2004) and Fig. 6 (right) shows the regression line between the two. With a value of $R^2 = 0.85$ for this crop and values between 0.48 and 0.87 for other crops, there is evidence that SWAT predicts the observed crop yields acceptably.

4.3. Calibration and verification of the QM-bias correction method

For the QM bias correction, the daily climate data of the reference period (1982–2004) are split into a (1982–1995) calibration and (1996–2004) verification group. A moving window with a length of 31 days centered on each calendar date is used to construct the ECDFs used in Eq. (12) to avoid abrupt inconsistencies (Thrasher et al., 2012; Dobler et al., 2012). The statistical results of the QM-calibration/verification task are listed in terms of R^2, NSE and IA in Table 5. Compared with the raw (uncorrected) GCM outputs, significant improvements obtained with the QM bias correction are immediately noticeable.

4.4. QM-bias correction downscaling for future scenarios/time periods

Assuming that the optimal bias-correction factor $CF_d^{GCM,\,ref}$ (Eq. (12)) computed for the reference (calibration) period applies also for the future, climate change in the KRB is predicted for two RCP's (RCP 4.5 and RCP 8.5) and two future time periods (2038–2060 and 2078–2100), with the results summarized in Table 6. For reference the average values of these climate variables the historic baseline period are shown in Fig. 7.

Table 6 indicates that the future changes of the mean temperature are all across the board positive with, averaged over the KRB, the most extreme increases of 1.2–3.3 °C experienced for the (expectedly) RCP8.5/2078–2100 scenario/period. Moreover, the highest temperature increases are predicted for the Qarasou and Seymareh sub-basins. Regarding the mean future precipitation in the KRB, the situation is more varied. Thus, there will be an increase under RCP 4.5/2038–2060 and RCP 8.5/2078–2100 scenarios/periods. However, in the northern zones (Gamasiab, Qarasou and Seymareh), RCP 4.5/2078–2100 and RCP 8.5/2038–2060 scenarios/periods predict a reduction of the precipitation, whereas in the south of the KRB a slight increase of the precipitation, ranging between 6% and 31%, will be experienced. Despite of this somewhat positive finding in this part of the KRB, the existence of mostly agricultural irrigated lands, population growth, and the mentioned rise in temperature with a subsequent increase of evaporation, may increase the risk of water scarcity.

It may be noted that Abbaspour et al. (2009) reported an increase of the future precipitation across Iran, particularly in its northern regions for various climate scenarios. For the KRB studied here, Vaghefi et al. (2015) investigated the climate change impacts on water resources using the downscaled climate predictors of the CGCM 3.1 version T63-

Table 8
Annual agricultural benefits obtained for the actual historic period and the three SLMP–optimized periods/scenarios (historic period and the two near-future climate scenarios).

Objective function	Actual historic	SLMP historic	RCP 4.5/2038–2060 (SLMP)	RCP 8.5/2038–2060 (SLMP)
Annual total benefit (million US$)	92.09	94.24	88.33	72.07

climate model with A1B, A2, and B1 SRES-scenarios for the period of 2020–2049 and found slight decreases in the projected monthly precipitation in the DA-and AZ-regions of the KRB for B1, and increases for A2.

4.5. SWAT-modelled climate change impacts on KRB-streamflow

Using the new bias-corrected climate data, the calibrated SWAT-model was built up and executed again for each future RCP-scenario. The 20-year mean monthly discharges for historical and future scenarios are presented in Fig. 8 for 5 gauging stations located at the end of the Gamasiab, Qarasou, Seymareh, Kashkan and South Karkheh sub-basins.

The various panels of the figure indicate that for all future scenarios (except RCP 4.5/2078–2100) the previously found general precipitation increase (see Table 6) will also lead to an increase of the river flow. On the other hand, as the wet seasons experience somewhat less precipitation, an associated decrease of the river flow is also observed. Compared with the baseline period, significant discharge decreases are expected under scenario RCP 4.5/2078–2100, due to the fact, that much less precipitation and higher temperatures (see Table 6) will occur. In particular, for the RCP 8.5/2078–2100 scenario, the monthly discharges in the Gamasiab and South Karkheh sub-basins show an increase of +300% in August and September and a reduction of −50% between March and May, i.e. the time period important for the first irrigation of wheat and barley crops. In the Kashkan and Seymareh sub-basins the corresponding seasonal changes are +100% and −80%. All scenarios/periods, except RCP 4.5/2078–2100, show similar trends. It should be noted that comparable large future changes in the streamflow ranging between −100% to +500% were found for some parts of KRB in the earlier mentioned study of Vaghefi et al. (2014). Nevertheless, for some KRB sub-basins, the RCP 4.5 scenario shows less average streamflow in the 2038–2060 than in the historical reference period. And this is, despite the fact that in Table 5 RCP 4.5/2038–2060 scenario/period experiences higher rainfall in the whole catchment. The reason is higher temperatures, leading to higher evapotranspiration, i.e. less surface water runoff. Similar tendencies of the effects of climate change on streamflow have also been found by Arias et al. (2014) in northwestern Spain.

4.6. Economic benefit analysis

4.6.1. Approach

Using the coupled SWAT-LINGO-MODSIM-PSO (SLMP) model (Fig. 4), the optimal irrigation schedule and cropping pattern for maximum annual profits are determined in five main agricultural regions in the south of the KRB for the baseline period, RCP 4.5/2038–2060 and RCP 8.5/2038–2060 scenarios/periods. For the MODSIM-PSO-model a constriction factor of 1, particle size of 40, ωmax and ωmin of 1.2 and 0.1, respectively, and a predefined maximum number of 100 iterations for finding the maximum of the cost function (16) was used. However, as Fig. 9 shows, for the RCP 4.5/2038–2060 scenario/period, convergence of the annual benefit towards a maximum (=negative minimum) is usually obtained already after about 20 iterations, with only minor changes in the cost function hereafter.

4.6.2. Estimation of optimal ratios of water allocation to potential crop water required

The allocated water to each crop in the five main agricultural plains in the south of the KRB - which is a function of the areas under cultivation (=decision variables) - as determined quasi as a "by-product" during the iterative annual benefit SLMP-maximization - is shown for the three scenarios/periods in Fig. 10. One can firstly notice prevalent crop water deficits for all crops in all three scenarios/periods, which are particularly high for maize and other crops and less so for the two crops wheat and barley, whose potential water requirements are met by about 77% in DA and 65% in AZ. This may be due to the fact that there is more rainfall during the months November to June which is the major growth season of wheat and barley. On the other hand, these results mean also that if the amount of irrigation water could be increased, maize cultivation would benefit the most.

For the two future scenarios/periods, Fig. 10 illustrates that for the wheat-, barley- and "other crops"- cultivation areas, the percentage ratios of allocated to potential water required will be systematically lower, but higher for the maize areas. One reason for this peculiar behavior could be the SWAT-predicted increases of streamflow discharge in the Karkheh-river in summer which is the major maize growth period and decreasing water discharge in the river in winter (see Fig. 8) which is the major wheat and barley growth period. Expectedly, for all four crops, the water deficits are the highest for the more extreme RCP 8.5 scenario. These results clearly indicate that the water scarcity predicted in the KRB for the near future may indeed adversely affect the crop yields in this agricultural plain.

4.6.3. Estimation of optimal crop areas and maximum total annual economic return

The future hydroclimate change manifesting itself as systematic crop water deficit has a direct effect on the percentage distribution of the various crop areas for maximization of the annual benefits in the KRB. This is shown in Fig. 11 which indicates that the percentage of optimum allocation of agricultural lands for wheat, barley, as well as "other crop" cultivation in all five agricultural areas will be less in the two future scenarios than for the reference period. In contrast, but in line with Fig. 10, for maize, the opposite holds, i.e. its cultivation area will be increased. Again, the changes are larger for the RCP 8.5 than the RCP 4.5 scenario. It is interesting to know how the present and future optimal crop areas computed by SLMP above compare with the projections of the local agricultural authorities. This is shown in Table 7 which lists the values of the optimal crop areas computed by SLMP for the three scenarios/periods in comparison with the authorities-projected future maximum and minimum crop cultivation areas. Compared with the historic period, the two future scenarios/period shows lower values for wheat and barley crop areas, but larger ones for maize. Moreover, the crop areas in the lower regions of the KRB, like AZ, tend towards the minimum of the allowable ranges, as less water allocation is experienced in these areas now and in the future (see also Fig. 10). Finally, the average annual economic benefits (=the objective function) obtained as probably the ultimate and most interesting result of the present optimization task are listed in Table 8. One can see that he total annual benefits will be significantly reduced from the present-day (baseline period) value of 94 million US$ to 88 and 72 Mill US$ for the RCP 4.5/2038–2060 and RCP 8.5/2038–2060 scenarios/period, i.e. a drop of about 20% for the latter case. This is indeed the price agriculture in the KRB has to pay for climate change in the near future. Interestingly, the second and third column of Table 8 indicate that even for the historic period the application of the SLMP-method results in optimized annual agricultural benefits which are about 2 million US$ higher than the actually projected ones (94 versus 92 million US$).

5. Summary and conclusions

In this study a comprehensive and integrated water management modeling tool, consisting of a combination of SWAT-LINGO-MODSIM-PSO (SLMP) was developed to allocate water to five important agricultural plains in the south of the KRB, such that the annual profit from all crops in the agricultural areas is maximized. This SLMP-model is applied to historic and future climate change scenarios to determine optimal cropping pattern for the historic and near-future period (2038–2060) under two RCP-climate scenarios.

Firstly, a SWAT-hydrological model was built and calibrated/validated on observed river streamflow along the Karkheh main river. The statistical measures show a good agreement between observed and simulated streamflows. The calibrated SWAT-model was then used further to estimate the annual crop yields as a function of water-availability using observed time series of wheat crop yields as calibration targets

and standard SWAT-crop parameters for other crops. Good agreements between simulated and observed crops yields are obtained.

Under the two climate change scenarios RCP 4.5 and RCP 8.5, daily future climate (precipitation, max/min temperature) data using the QM bias correction downscaling method were predicted for the future time periods 2038–2060 and 2078–2100. The advantage of the QM method could be demonstrated by significant statistical improvements in the adjustments of the predicted to the observed climate variables in the historical period 1982–2004. The calibrated SWAT-model was then run to estimate the river discharge under the projected climate change scenarios in five important sub-basins of the KRB. Most future scenario projections follow a similar trend, though with different percentage changes. Overall, the future river flow is predicted to increase during the dry season and to decrease in the wet season. The inflow time series to the Karkheh reservoir extracted from SWAT for the different scenarios/periods were then entered into MODSIM for water allocation modeling, i.e. to distribute the available water to different crops in the five agricultural regions under SOP rules in a reservoir-irrigation system - which turns out to be under permanent water deficit - to determine the optimal agricultural cultivation pattern.

For the final economic optimization of this water-limited agricultural system, MODSIM was linked to PSO to maximize the annual benefits, considering the impacts of water shortage on crop yields, wherefore the latter were maximized using the LINGO-optimization module embedded in MODSIM-PSO. This completes the build-up of the SLMP-model which was then run in an iterative process for the historic and two near-future (RCP 4.5/2038–2060 and RCP 8.5/2038–2060) climate scenarios to find the best combination of areas under cultivation to maximize the annual profit. As a final result a total annual profit of 88 million US$ and 72 million US$ is obtained for RCP 4.5/2038–2060 and RCP 8.5/2038–2060 climate scenarios, respectively, which has to be compared with the 94 million US$ income for present baseline period. In fact, this income decrease is mainly due to a substantial increase of (low price) maize-covered areas, as a summer growing crop, and a decrease of cultivation areas devoted to (high price) wheat and barley as cold weather crops in the future.

In conclusion, the results of this study indicate that:

1- The SLMP-model is a practical and viable tool for an economic analysis and optimization in an irrigated, agriculturally used watershed in the wake of climate change, thus providing local water authorities a perspective for decision-making and future planning of limited agricultural resources.

2- The way, the SLMP-model is integrated, it is easy to apply and can be a handy decision tool for economic optimal allocation of agricultural water, especially, in irrigation-water-limited areas.

3- Using the network flow programming algorithm embedded in MODSIM for water allocation and the PSO algorithm to find the global optimal solutions, makes the SLMP-model fast and efficient for the maximization of agricultural benefits.

References

Abbaspour, K.C., Johnson, C.A., Van Genuchten, M.T., 2004. Estimating uncertain flow and transport parameters using a sequential uncertainty fitting procedure. Vadose Zone J. 3 (4), 1340–1352.

Abbaspour, K.C., Yang, J., Maximov, I., Siber, R., Bogner, K., Mieleitner, J., Zobrist, J., Srinivasan, R., 2007. Modelling hydrology and water quality in the pre-alpine/alpine Thur watershed using SWAT. J. Hydrol. 333 (2), 413–430.

Abbaspour, K.C., Faramarzi, M., Ghasemi, S.S., Yang, H., 2009. Assessing the impact of climate change on water resources in Iran. Water Resour. Res. 45 (10).

Ahmad, M.U.D., Giordano, M., 2010. The Karkheh River basin: the food basket of Iran under pressure. Water Int. 35 (5), 522–544.

Allen, M.R., Ingram, W.J., 2002. Constraints on future changes in climate and the hydrologic cycle. Nature 419 (6903), 224–232.

Altunkaynak, A., Özger, M., Çakmakci, M., 2005. Water consumption prediction of Istanbul city by using fuzzy logic approach. Water Resour. Manag. 19 (5), 641–654.

Amiri, M.J., Eslamian, S.S., 2010. Investigation of climate change in Iran. J. Environ. Sci. Technol. 3 (4), 208–216.

Arias, R., Rodríguez-Blanco, M.L., Taboada-Castro, M.M., Nunes, J.P., Keizer, J.J., Taboada-Castro, M.T., 2014. Water resources response to changes in temperature, rainfall and CO_2 concentration: a first approach in NW Spain. Water 6 (10), 3049–3067.

Arnold, J.G., Srinivasan, R., Muttiah, R.R., Williams, J.R., 1998. Large area hydrologic modeling and assessment—part 1: model development. J. Am. Water Resour. Assoc. 34 (1), 73–89.

Banihabib, M.E., Hosseinzadeh, M., Peralta, R.C., 2016. Optimization of inter-sectorial water reallocation for arid-zone megacity-dominated area. Urban Water J. 13 (8), 852–860.

Baumgart, P., 2005. Lower green bay and lower fox tributary modeling report. Prepared for Oneida Tribe of Indians of Wisconsin and Green Bay Remedial Action Plan Science and Technical Advisory Committee.

Bertsekas, D.P., Tseng, P., 1994. "RELAX-IV: A faster version of the RELAX code for Solving minimum cost flow problems", Technical Report P-2276. Massachusetts Institute of Technology, Laboratory for Information and Decision Systems.

Betts, R.A., Golding, N., Gonzalez, P., Gornall, J., Kahana, R., Kay, G., Mitchell, L., Wiltshire, A., 2015. Climate and land use change impacts on global terrestrial ecosystems and river flows in the HadGEM2-ES Earth system model using the representative concentration pathways. Biogeosciences 12:1317–1338. https://doi.org/10.5194/bg-12-1317-2015, 2015.

Caesar, J., Palin, E., Liddicoat, S., Lowe, J., Burke, E., Pardaens, A., Sanderson, M., Kahana, R., 2013. Response of the HadGEM2 Earth System Model to future greenhouse gas emissions pathways to the year 2300. J. Clim. 26 (10), 3275–3284.

Calzadilla, A., Rehdanz, K., Tol, R.S., 2010. The economic impact of more sustainable water use in agriculture: a computable general equilibrium analysis. J. Hydrol. 384 (3), 292–305.

Collins, W.J., Bellouin, N., Doutriaux-Boucher, M., Gedney, N., Halloran, P., Hinton, T., Hughes, J., Jones, C.D., Joshi, M., Liddicoat, S., Martin, G., 2011. Development and evaluation of an Earth-System model-HadGEM2. Geosci. Model Dev. 4 (4), 1051.

Dobler, C., Hagemann, S., Wilby, R.L., Stötter, J., 2012. Quantifying different sources of uncertainty in hydrological projections in an Alpine watershed. Hydrol. Earth Syst. Sci. 16 (11), 4343–4360.

Doorenbos, J., Kassam, A.H., 1979. Yield Response to Water. FAO Irrigation and Drainage Paper No. 33. Rome, Italy.

Eberhart, R., Kennedy, J., 1995, October. A new optimizer using particle swarm theory. Micro Machine and Human Science, 1995. MHS'95., Proceedings of the Sixth International Symposium on. IEEE, pp. 39–43.

Eberhart, R., Shi, Y., 1998. Comparison between genetic algorithms and particle swarm optimization. Evolutionary Programming VII. Springer Berlin, Heidelberg, pp. 611–616.

Fereidoon, M., Koch, M., 2016. SWAT-model based identification of watershed components in a semi-arid region with long term gaps in the climatological parameters' database. Proceedings of SGEM Vienna GREEN, Vienna, Austria, November 2–5, 2016.

Fereidoon, M., Koch, M., 2017. SWAT-modeling of the effects of the construction of a dam on streamflow in the Karkheh Basin, Iran. Journal of Thai Interdisciplinary Research 12 (4):79–86. https://doi.org/10.14456/jtir.2017.32.

Fischer, G., Shah, M., Tubiello, F.N., Van Velhuizen, H., 2005. Socio-economic and climate change impacts on agriculture: an integrated assessment, 1990–2080. Philos. Trans. R. Soc., B 360 (1463), 2067–2083.

Food and Agriculture Organization (FAO), 1995. The digital soil map of the world and derived soil properties, version 3.5 (CD-ROM), Rome.

Gassman, P.W., Sadeghi, A.M., Srinivason, R., 2014. Applications of the SWAT model special section: overview and insights. J. Environ. Qual. 43 (1), 1–8.

Hendricks, N.P., Peterson, J.M., 2012. Fixed effects estimation of the intensive and extensive margins of irrigation water demand. J. Agric. Resour. Econ. 1–19.

Jones, C., Lowe, J., Liddicoat, S., Betts, R., 2009. Committed terrestrial ecosystem changes due to climate change. Nat. Geosci. 2 (7), 484–487.

Kang, Y., Khan, S., Ma, X., 2009. Climate change impacts on crop yield, crop water productivity and food security—a review. Prog. Nat. Sci. 19 (12), 1665–1674.

Khan, S., Hanjra, M.A., Mu, J., 2009. Water management and crop production for food security in China: a review. Agric. Water Manag. 96 (3), 349–360.

Koch, M., Cherie, N., 2013. SWAT modeling of the impact of future climate change on the hydrology and the water resources in the upper Blue Nile River basin, Ethiopia. Proceedings of the 6th International Conference on Water Resources and Environment Research, ICWRER. vol. 6, No. 6, pp. 488–523.

Kundu, S., Khare, D., Mondal, A., 2017. Individual and combined impacts of future climate and land use changes on the water balance. Ecol. Eng. 105, 42–57.

Labadie, J., 1995. MODSIM: River basin network flow model for conjunctive stream-aquifer management. Program User Manual and Documentation. Colorado State University, Ft. Collins, CO.

Larson, R.K., Spinazola, J., 2000. Conjunctive management analyses for endangered species flow augmentation alternatives in the Snake River. Watershed Management and Operations Management 2000, pp. 1–7.

Lenderink, G., Van Meijgaard, E., 2010. Linking increases in hourly precipitation extremes to atmospheric temperature and moisture changes. Environ. Res. Lett. 5 (2), 025208.

Madani, K., AghaKouchak, A., Mirchi, A., 2016. Iran's socio-economic drought: challenges of a water-bankrupt nation. Iran. Stud. 49 (6), 997–1016.

Marjanizadeh, S., de Fraiture, C., Loiskandl, W., 2010. Food and water scenarios for the Karkheh River Basin, Iran. Water Int. 35 (4), 409–424.

Marques, G.F., Lund, J.R., Leu, M.R., Jenkins, M., Howitt, R., Harter, T., Hatchett, S., Ruud, N., Burke, S., 2006. Economically driven simulation of regional water systems: Friant-Kern, California. J. Water Resour. Plan. Manag. 132 (6), 468–479.

Maurer, E.P., 2010. The utility of daily large-scale climate data in the assessment of climate change impacts on daily streamflow in California. Hydrol. Earth Syst. Sci. 14, 1125–1138.

Molden, D., 2007. Comprehensive assessment of water management in agriculture. Water for Food, Water for Life: A Comprehensive Assessment of Water Management in Agriculture. Earthscan and Colombo: International Water Management Institute, London.

Molle, F., Berkoff, J., 2009, February. Cities vs. agriculture: A review of intersectoral water re-allocation. Natural Resources Forum. vol. 33, No. 1. Blackwell Publishing Ltd., pp. 6–18.

Moore, M.R., Gollehon, N.R., Carey, M.B., 1994. Multicrop production decisions in western irrigated agriculture: the role of water price. Am. J. Agric. Econ. 76 (4), 859–874.

Moriasi, D.N., Arnold, J.G., Van Liew, M.W., Bingner, R.L., Harmel, R.D., Veith, T.L., 2007. Model evaluation guidelines for systematic quantification of accuracy in watershed simulations. Trans. ASABE 50 (3), 885–900.

Muthuwatta, L.P., Ahmad, M.U.D., Bos, M.G., Rientjes, T.H., 2010. Assessment of water availability and consumption in the Karkheh River Basin, Iran—using remote sensing and geo-statistics. Water Resour. Manag. 24 (3), 459–484.

Neitsch, S.L., Arnold, J.C., Kiniry, J.R., Williams, J.R., King, K.W., 2002. Soil and Water Assessment Tool Theoretical Documentation. Version 2000. Texas Water Resources Institute, College Station, TX.

Parsopoulos, K.E., Vrahatis, M.N., 2002. Recent approaches to global optimization problems through particle swarm optimization. Nat. Comput. 1 (2–3), 235–306.

Qureshi, A.S., Oweis, T., Karimi, P., Porehemmat, J., 2010. Water productivity of irrigated wheat and maize in the Karkheh River basin of Iran. Irrig. Drain. 59 (3), 264–276.

Reder, A., Rianna, G., Vezzoli, R., Mercogliano, P., 2016. Assessment of possible impacts of climate change on the hydrological regimes of different regions in China. Adv. Clim. Chang. Res. 7 (3), 169–184.

Schmalz, B., Fohrer, N., 2009. Comparing model sensitivities of different landscapes using the ecohydrological SWAT model. Adv. Geosci. 21, 91–98.

Sethi, L.N., Panda, S.N., Nayak, M.K., 2006. Optimal crop planning and water resources allocation in a coastal groundwater basin, Orissa, India. Agric. Water Manag. 83 (3), 209–220.

Srinivasan, R., Zhang, X., Arnold, J., 2010. SWAT ungauged: hydrological budget and crop yield predictions in the Upper Mississippi River Basin. Trans. ASABE 53 (5), 1533–1546.

Stewart, J.I., Robert, M.H., 1973. Functions to predict effects of crop water deficits. J. Irrig. Drain. Div. 99 (4), 421–443.

Sulis, A., Sechi, G.M., 2013. Comparison of generic simulation models for water resource systems. Environ. Model. Softw. 40, 214–225.

Taylor, K.E., Stouffer, R.J., Meehl, G.A., 2012. An overview of CMIP5 and the experiment design. Bull. Am. Meteorol. Soc. 93 (4), 485–498.

Teutschbein, C., Seibert, J., 2012. Bias correction of regional climate model simulations for hydrological climate-change impact studies: review and evaluation of different methods. J. Hydrol. 456–457:12–29. https://doi.org/10.1016/j.jhydrol.2012.05.052.

Themeßl, M.J., Gobiet, A., Heinrich, G., 2012. Empirical-statistical downscaling and error correction of regional climate models and its impact on the climate change signal. Clim. Chang. 112 (2), 449–468.

Thrasher, B., Maurer, E.P., McKellar, C., Duffy, P.B., 2012. Bias correcting climate model simulated daily temperature extremes with quantile mapping. Hydrol. Earth Syst. Sci. 16 (9), 3309–3314.

Ullrich, A., Volk, M., 2009. Application of the Soil and Water Assessment Tool (SWAT) to predict the impact of alternative management practices on water quality and quantity. Agric. Water Manag. 96 (8), 1207–1217.

Usman, M., 2016. Contribution of agriculture sector in the GDP growth rate of Pakistan. J. Glob. Econ. 4 (184):2. https://doi.org/10.4172/2375-4389.1000184.

Vaghefi, S.A., Mousavi, S.J., Abbaspour, K.C., Srinivasan, R., Yang, H., 2014. Analyses of the impact of climate change on water resources components, drought and wheat yield in semiarid regions: Karkheh River Basin in Iran. Hydrol. Process. 28 (4), 2018–2032.

Vaghefi, S.A., Mousavi, S.J., Abbaspour, K.C., Srinivasan, R., Arnold, J.R., 2015. Integration of hydrologic and water allocation models in basin-scale water resources management considering crop pattern and climate change: Karkheh River Basin in Iran. Reg. Environ. Chang. 15 (3), 475–484.

Varanou, E., Gkouvatsou, E., Baltas, E., Mimikou, M., 2002. Quantity and quality integrated catchment modeling under climate change with use of soil and water assessment tool model. J. Hydrol. Eng. 7 (3), 228–244.

Wang, Z., Yang, J., Deng, X., Lan, X., 2015. Optimal water resources allocation under the constraint of land use in the Heihe River Basin of China. Sustainability 7 (2), 1558–1575.

Wilby, R.L., Dawson, C.W., 2013. The Statistical DownScaling Model (SDSM): insights from one decade of application. Int. J. Climatol. 33, 1707–1719.

Wood, A.W., Leung, L.R., Sridhar, V., Lettenmaier, D.P., 2004. Hydrologic implications of dynamical and statistical approaches to downscaling climate model outputs. Clim. Change 62 (1–3):189–216. https://doi.org/10.1023/B: CLIM.0000013685.99609.9e.

Zare, M., Koch, M., 2014. Optimization of cultivation pattern for maximizing farmers' profits under land-and water constraints by means of linear programming: an Iranian case study. 11th International Conference on Hydroscience & Engineering. Hamburg, ICHE.

Zare, M., Koch, M., 2017. Conjunctive management of surface-groundwater resources by coupling a hybrid Wavelet-ANFIS/Fuzzy C-means (FCM) clustering model with particle swarm optimization (PSO): application to the Miandarband Plain, Iran. Agric. Water Manag. (unpublished results).

Zhou, S.L., McMahon, T.A., Walton, A., Lewis, J., 2002. Forecasting operational demand for an urban water supply zone. J. Hydrol. 259 (1), 189–202.